Optical Property Estimation by Precomputed Tensor Method for High-fidelity SRP Model

By Satoshi Ikari,[1)] Kakeru Tokunaga,[1)] Takahiro Ito,[2)] Takaya Inamori,[3)] Ryu Funase,[1)] and Shinichi Nakasuka[1)]

[1)]*Department of Aeronautics and Astronautics, The University of Tokyo, Tokyo, Japan*
[2)]*Institute of Space and Astronautical Science, JAXA, Sagamihara, Japan*
[2)]*Department of Micro-Nano System Engineering , Nagoya University, Nagoya, Japan*

Solar Radiation Pressure (SRP) is a major disturbance of high altitude earth orbiting satellites and interplanetary spacecraft. In order to analyze the precise motion of orbit or attitude of these space vehicles, a high-fidelity SRP model was widely studied by several researchers. Practical astrodynamics analyses require not only the accuracy but also the fast calculation and model correction capabilities because given numerical models always have some uncertainties or mismodeling. This paper proposes an accurate, fast, and model correctable SRP calculation method by using the precomputed tensors which are obtained from only the spacecraft geometry model. The proposed method decomposes and reconstructs the SRP equation to satisfy the three conflicting requirements. Furthermore, the proposed model was evaluated by using real flight data in this paper. The evaluation results revealed that the proposed method can improve the modeling accuracies and accelerate the calculation cost.

Key Words: Disturbance modelling, Solar Radiation Pressure, and Optical property estimation

Nomenclature

$d_{S\odot}$	:	distance between sun and spacecraft
$\boldsymbol{i}$	:	sun direction vector at body-fixed frame
$\boldsymbol{l}$	:	position vector at body-fixed frame
$\boldsymbol{n}$	:	normal vector at body-fixed frame
t	:	time
A	:	are
C_a	:	solar absorption ratio
C_s	:	solar specular reflection ratio
C_d	:	solar diffuse reflection ratio
$\boldsymbol{F}$	:	solar radiation force at body-fixed frame
$\boldsymbol{L}$	:	angular momentum at body-fixed frame
$P_\odot$	:	solar radiation pressure at 1AU $P_\odot = 4.56 \times 10^{-6}\ \mathrm{N/m^2}$
$\boldsymbol{T}$	:	solar radiation torque at body-fixed frame

Subscripts

b	:	body-fixed frame ($b = 1,2,3 = x,y,z$)
k	:	index of basis function ($k = 1,2 \cdots K$)
o	:	index of observation
p	:	index of micro-surfaces ($p = 1,2 \cdots P$)
ϖ	:	pseudo body-fixed frame for torque tensor expression ($\varpi = 1,2,3 = x,y,z$)

Diacritics

$\bar{(\ )}$	:	center of mass

1. Introduction

Solar Radiation Pressure (SRP) is a major disturbance force and torque for spacecraft in high altitude earth orbits and in interplanetary orbits. For an accurate SRP calculation, a high-fidelity geometry model is needed, and effects of shadows on the surfaces casted by other surfaces should be computed by using a time consuming calculation method. Thus, there is a trade-off relationship between the accuracy and the calculation cost. In addition, for a practical usage, a parameter estimation method is required to represent the actual on-orbit behavior because given numerical models always have some mismodeling or uncertainties in their own parameters (e.g., optical properties, solar paddle angle, center of mass, or others). Therefore, an accurate, fast, and model correctable SRP calculation method is required for practical astrodynamics analyses such as precise orbit determination for navigation satellites or attitude analysis for deep space probes.

For accurate and fast SRP calculation, recent researchers have proposed several approximation methods. In these methods, accurate SRP forces or torques of certain sun vectors are precomputed, and the data set of the forces or torques is stored as a data table or is expanded to coefficients corresponding to a certain function as an approximation [1], [2], [3]. Although the table or the approximated coefficients can be used to compute accurate SRP in a short computation time, the methods cannot directly estimate the physics parameters in the given model. These methods can correct the approximated coefficients to fit on-orbit results. However, the coefficients are not suitable for the estimation because they do not have any constraints (e.g., the number of coefficients and the limitation of their value). On the other hand, an optical property estimation method has been discussed, but these methods focus on low-fidelity geometry models and do not consider the shadow effect [4]. In fact, a SRP calculation method which achieve the three requirement (i.e., accurate,

fast, and model correctable) is not yet proposed.

In order to construct an accurate, fast, and model correctable SRP calculation method, S. Ikari *et al.* have proposed the precomputed tensor method [5], [6]. The key techniques of the proposed method are decomposition and reconstruction of three components for the SRP calculation: spacecraft geometry, a material reflection property, and the sun information. Each of the components has different properties of information quantity, time variation, and uncertainty. These properties are important for fast calculation and parameter estimation. Conventional methods cannot effectively use these different properties because they integrate the three components in the surface integral process. By using the idea of the decomposition and the reconstruction, the proposed method can precompute the time consuming ray-trace computation and surface integral by using only geometry model of the spacecraft, and several precomputed tensors are generated. Finally, by using the precomputed tensors, an accurate and fast SRP equation and a linearized equation for the optical property estimation can be derived.

Furthermore, in this study, for verification of the effect of the proposed method, on-orbit spacecraft analysis was performed. Flight data of PROCYON [7], which is a 50-kg class interplanetary micro-spacecraft is analyzed. The precomputed tensors for the proposed method are calculated from the 3D geometry model of the PROCYON by using the tensor calculation tool developed by authors. This paper introduces a process of the precomputed tensor calculation, a method for the optical property estimation, and the result of the angular momentum analysis by using the on-orbit data of PROCYON.

2. Proposed SRP Calculation Method

2.1. Three components for SRP calculation

For a SRP calculation, a spacecraft geometry, a material reflection property, and the sun information are needed. A spacecraft geometry model is expressed as an assemblage of micro-surfaces, and the center of mass position vector are defined for the spacecraft. Each micro-surface has material information and three geometrical properties: the normal vector, the position vector, and the area of the surface. The number of the micro-surfaces is proportional to the fidelity of the geometry model. For the material reflection property, we assume that the interaction between light and materials can be expressed by three behaviors: the absorption, the specular reflection, and the Lambertian diffuse reflection. The ratios of these behaviors are defined as optical properties C_a, C_s, and C_d, and the sum of them will be one since the energy conservation law. Each material has the optical properties in the sun light spectrum. The sun position vector in the body-fixed frame is given as an input for a SRP calculation. The distance between the sun and the spacecraft is varied by the orbital motion of the spacecraft, and the direction between them is varied by the attitude motion of the spacecraft.

Each of the three components has different properties shown in Table 1. It is assumed that spacecraft geometry models which can be obtained from CAD data is almost fixed and low uncertainty, expect a rotatable solar paddle. However, the model has huge quantity of information. Optical properties are gradually varied by the space aging effect and have large uncertainty. The sun distance from spacecraft is varied by orbital motion, and the sun direction in the body-fixed frame is varied by attitude motion of the spacecraft. These motions are fast but can be determined by using other sensors or systems. In order to construct an accurate, fast, and model correctable SRP calculation method, the three components should be decomposed and reconstructed with respect to each property. The decomposition and reconstruction technique for the proposed method will be discussed in next subsection.

Table 1. Properties of three components for SRP calculation

	Information quantity	Time variation period	Uncertainty
Spacecraft geometry	High	Fixed	Low
Optical property	Low	Slow	Large
Sun position	Low	Fast	Low

2.2. Basic equation of SRP torque acting on spacecraft

Under the problem setting described above, the SRP force acting on a micro-surface p is obtained as follows:

$$\boldsymbol{F}_p = -P_{d_{S\odot}} A_p V_p(\boldsymbol{i})(\boldsymbol{i}\cdot\boldsymbol{n}_p)\left[\boldsymbol{i} + C_{s_p}\{2(\boldsymbol{i}\cdot\boldsymbol{n}_p)\boldsymbol{n}_p - \boldsymbol{i}\} + \frac{2}{3}C_{d_p}\boldsymbol{n}_p\right], \tag{1}$$

where $P_{d_{S\odot}}$ is a solar radiation force density function and defined as following equation:

$$P_{d_{S\odot}} = \left(\frac{1\mathrm{AU}}{d_{S\odot}}\right)^2 P_{\odot}. \tag{2}$$

$V_p(\boldsymbol{i})$ is the binary visibility function, which represents the shadows on the micro-surface casted by other surfaces. $V_p(\boldsymbol{i})$ is defined on the unit sphere at the body-fixed frame as follows:

$$V_p(\boldsymbol{i}) = \begin{cases} 1 & \text{ray from } \boldsymbol{i} \text{ hit the surface } p \\ 0 & \text{ray from } \boldsymbol{i} \text{ doesn't hit the surface } p \end{cases}. \tag{3}$$

The SRP torque acting on the spacecraft is computed as a total amount of the torque of all micro-surfaces as follows:

$$\begin{aligned} \boldsymbol{T} &= \sum_{p=1}^{P}\{(\boldsymbol{l}_p - \bar{\boldsymbol{l}}) \times \boldsymbol{F}_p\} \\ &= \sum_{p=1}^{P}(\boldsymbol{l}_p \times \boldsymbol{F}_p) - \bar{\boldsymbol{l}} \times \boldsymbol{F}. \end{aligned} \tag{4}$$

Most conventional SRP models firstly computes the shadow effect by using ray-tracing method and calculates the SRP torques acting on each micro-surface. After that, the total SRP torque is output by using Eq. (4). If the geometry model has Pth micro-surfaces, the calculation cost of the ray-tracing is $O(P^2)$, and the calculation cost of total SRP torque is $O(P)$. The number of surfaces P reaches 10^5 orders for high-fidelity spacecraft geometry model. Therefore, the calculation cost is too high to be used in practical analyses. To decrease the calculation cost, conventional high-fidelity SRP

calculation methods precomputes the total SRP torque (or force) and directly approximates the torque by using an arbitrary basis function $\vartheta_k(\boldsymbol{i})$ as follows:

$$\boldsymbol{T} = c_1\vartheta_1(\boldsymbol{i}) + c_2\vartheta_2(\boldsymbol{i}) + \cdots. \tag{5}$$

Although these torque (or force) approximation methods can accurately and quickly calculate the SRP, they do not suit for a model correction because the parameters $c_1, c_2, \cdots$ have no physical meaning. For example, the number of the parameters or constraints of the values cannot be decided theoretically. On the other hands, the proposed method approximates more primitive function instead of the final output of the SRP torque. This primitive approximation allows us the decomposition of the three components, and finally, a linearized SRP equation that can estimate optical properties, is derived.

2.3. Derivation of proposed method

This subsection introduces the derivation process of the proposed SRP calculation method, especially, for SRP torque. The proposed model for SRP force has been discussed in the Ref. [6]. As mentioned above, approximation of a primitive function is a key of this method. The proposed method approximates the binary visibility function of each micro-surface $V_p(\boldsymbol{i})$. The function can be computed with only the spacecraft geometry model that is a fixed, and its calculation cost is very high. Therefore, the precomputation and approximation of the visibility function is effective to construct a fast calculation method. The approximation is performed as follows:

$$\begin{aligned} V_p(\boldsymbol{i}) &\cong v_{p1}\varphi_1(\boldsymbol{i}) + \cdots + v_{pK}\varphi_K(\boldsymbol{i}) \\ &= [v_{p1} \quad \cdots \quad v_{pK}]\begin{bmatrix}\varphi_1(\boldsymbol{i}) \\ \vdots \\ \varphi_K(\boldsymbol{i})\end{bmatrix} = \boldsymbol{v}_p\boldsymbol{\varphi}(\boldsymbol{i}), \end{aligned} \tag{6}$$

where v_{pk} is the approximation coefficient, and $\varphi_k(\boldsymbol{i})$ is arbitrary basis function defined on the unit sphere at body-fixed frame. In this paper, the spherical Haar wavelet [8] is chosen for the basis function because it is suitable for an approximation of a discrete function such as $V_p(\boldsymbol{i})$. Actually, according to our simulation results, it can provide more accurate and faster SRP calculation [5].

Equation (6) shows that the approximation can be expressed as an inner product of the coefficients vector and the basis function vector. Additionally, the cross product of the position vector $\boldsymbol{l}$ in Eq. (4) can be expressed as 2nd-rank tensor $l_{\varpi b}$ as following equation:

$$\boldsymbol{T} = \boldsymbol{l} \times \boldsymbol{F} \iff T_\varpi = \begin{bmatrix} 0 & -l_3 & l_2 \\ l_3 & 0 & -l_1 \\ -l_2 & l_1 & 0 \end{bmatrix}\begin{bmatrix}F_1 \\ F_2 \\ F_3\end{bmatrix} = l_{\varpi b}F_b \tag{7}$$

Therefore, we can use the calculus of tensors for a decomposition and reconstruction of the SRP equation. Hereafter, vectors in the SRP equation can be handled as 1st-rank tensors, and tensor calculus rules are applied similar with our previous studies [5], [6]. The tensor calculus rules deform the Eq. (1) to the following equation:

$$\begin{aligned} \boldsymbol{F}_p &= F_{pb} \\ &= -P_{d_{S\odot}}\tau_{pkb'}\left[i_b + C_{s_p}s_{pbb}i_b + \frac{2}{3}C_{d_p}n_{pb}\right]\varphi_k(i_b)i_{b'} \end{aligned} \tag{8}$$

where subscription b and b' both denote the body-fixed frame, but they are expressly used differently to protect the miscalculation in the commutative law of tensors. $\tau_{pkb'}$ and s_{pbb} are defined as follows:

$$\tau_{pkb'} = A_p v_{pk} n_{pb'}, \tag{9}$$

$$\begin{aligned} s_{pbb} &= 2n_{pbb} - I_{bb} \\ &= 2\begin{bmatrix} n_{p1}^2 & n_{p1}n_{p2} & n_{p1}n_{p3} \\ n_{p1}n_{p2} & n_{p2}^2 & n_{p2}n_{p3} \\ n_{p1}n_{p3} & n_{p2}n_{p3} & n_{p3}^2 \end{bmatrix} - \begin{bmatrix}1 & 0 & 0 \\ 0 & 1 & 0 \\ 0 & 0 & 1\end{bmatrix}. \end{aligned} \tag{10}$$

The SRP torque acting on a micro-surface p is derived as follows by using the tensor expression:

$$\begin{aligned} \boldsymbol{T}_p &= T_{p\varpi} \\ &= -P_{d_{S\odot}}l_{p\varpi b}\tau_{pkb'}\left[i_b + C_{s_p}s_{pbb}i_b + \frac{2}{3}C_{d_p}n_{pb}\right]\varphi_k(i_b)i_{b'}. \end{aligned} \tag{11}$$

Since the three components (i.e., spacecraft geometry, optical property, and sun information) are decomposed as tensors, the equation can be freely reconstructed in the micro-surface summation process (i.e., surface integral process). In this study, the SRP equation is reconstructed focusing on material group for the optical property estimation. Due to the first term of Eq. (11) is independent of materials, micro-surface summation is normally executed, and the 4th-rank tensor is generated as follows:

$$W_{\varpi bkb'} = \sum_{p=1}^{P} l_{\varpi b}\tau_{pkb'}. \tag{12}$$

The second and third terms of Eq. (11) depends on materials, thus the micro-surface summations are performed for each material as following equations:

$$Zs_{m\varpi kb'b} = \sum_{p_m} l_{\varpi b}\tau_{pkb'}\, s_{pbb}, \tag{13}$$

$$Zd_{m\varpi kb'} = \sum_{p_m} l_{\varpi b}\tau_{pkb'}\, n_{pb}, \tag{14}$$

where p_m denotes the set of surfaces made by the material m. These reconstructions derive the proposed SRP torque equation as follows:

$$\begin{aligned} \boldsymbol{T} &= T_\varpi \\ &= -P_{d_{S\odot}}\left[W_{\varpi bkb'}i_b + \left(\sum_{m=1}^{M} C_{s_m}Zs_{m\varpi kb'b}\right)i_b + \frac{2}{3}\sum_{m=1}^{M} C_{d_m}Zd_{m\varpi kb'}\right]i_{b'}\varphi_k(i_b) - \bar{l}_{\varpi b}F_b \end{aligned} \tag{15}$$

The three tensors $W_{\varpi bkb'}$, $Zs_{m\varpi kb'b}$, and $Zd_{m\varpi kb'}$ are generated by using only geometry information. Hence they can be precomputed and stored before the real time calculation, and only simple linear algebraic operations are executer in the real calculation phase. The theoretical calculation cost of Eq. (15) is $O(MK)$, where M is number of materials, and K is number of basis functions. The calculation cost no longer relates to the number of micro-surfaces P, thus the trade-off relationship between the accuracy and the calculation cost is resolved by using the precomputed tensors. Furthermore, Eq. (15) is a linearized equation for the optical properties C_{s_m} and C_{d_m} if the

precomputed tensors and the sun information are given. Hence, the optical properties can be estimated by using Eq. (15).

3. Optical Property Estimation

3.1. Time integration of SRP torque

This section describes the optical property estimation algorithm by using the proposed SRP calculation method. The optical properties can be estimated from both the orbital and attitude motion of the spacecraft. In this paper, for the PROCYON analysis, the estimation from the attitude motion is discussed. We assume that the spacecraft attitude is fixed to the inertial frame during one observation term, and the angular momentum at the body-fixed frame L_ϖ is observed from the telemetry of the reaction wheels. If the SRP torque is the only disturbance acting on the spacecraft, the following equation is derived according to the equation of rotation:

$$\boldsymbol{L} = \int \boldsymbol{T}\mathrm{d}t. \tag{16}$$

The angular momentum is discretely observed, and the Eq. (16) is expanded as follows by using the trapezoidal integration:

$$\boldsymbol{L}_{O'} = \frac{1}{2}\sum_{o=1}^{O'}[(t_o - t_{o-1})(\boldsymbol{T}_o + \boldsymbol{T}_{o-1})] + \boldsymbol{L}_0. \tag{17}$$

As mentioned in the previous section, the SRP torque $\boldsymbol{T}$ is a function of the three components. The spacecraft geometry is expressed by the precomputed tensors and assumed as constant values. The material information is expressed as optical properties and is handled as estimated values. Thus, the time variable value is only the sun information (i.e., sun distance and sun direction), and it can be obtained from the on-board sensor information and the determined orbit information. The time integral of the SRP torque is deformed to the time integral of the sun information tensor $\boldsymbol{\Theta}_{kbb'}$ and $\boldsymbol{\Psi}_{kb'}$ as following equations:

$$\begin{aligned}\boldsymbol{L}_{O'} = \boldsymbol{L}_0 - \frac{1}{2}\Bigg[& W_{\varpi bkb'}\boldsymbol{\Theta}_{kbb'_{O'}} \\ & + \boldsymbol{\Theta}_{kbb'_{O'}}\sum_{m=1}^{M} C_{s_m} Zs_{m\varpi bkb'} \\ & + \frac{2}{3}\boldsymbol{\Psi}_{kb'_{O'}}\sum_{m=1}^{M} C_{d_m} Zd_{m\varpi kb'}\Bigg],\end{aligned} \tag{18}$$

$$\boldsymbol{\Theta}_{kbb'_{O'}} = \sum_{o=1}^{O'}\left[(t_o - t_{o-1})\left(\theta_{kbb'_o} + \theta_{kbb'_{o-1}}\right)\right], \tag{19}$$

$$\theta_{kbb'_o} = P_{d_{S\odot_o}} i_{b_o} i_{b'_o} \varphi_k\left(i_{b_o}\right), \tag{20}$$

$$\boldsymbol{\Psi}_{kb'_{O'}} = \sum_{o=1}^{O'}\left[(t_o - t_{o-1})\left(\psi_{kb'_o} + \psi_{kb'_{o-1}}\right)\right], \tag{21}$$

$$\psi_{kb'_o} = P_{d_{S\odot_o}} i_{b'_o} \varphi_k\left(i_{b_o}\right). \tag{22}$$

Note that in the Eq. (18), the position vector of the center of mass is assumed as $\mathbf{0}$ for a simplification; however the expansion to include the center of mass can be derived as similar process.

3.2. Normal equation for linear least-squares method

A normal equation for the linear least-squares method to estimate the optical properties can be derived from Eq. (18). In this paper, not only the optical properties but also the initial angular momentum is considered as estimated values. When the observed angular momentum is obtained as $\boldsymbol{L}_o$, the normal equation is derived as following equations:

$$\begin{aligned}&\boldsymbol{y} = \boldsymbol{\mathcal{A}}\boldsymbol{x} \\ &\boldsymbol{y} = [\tilde{\boldsymbol{L}}_1 \quad \cdots \quad \tilde{\boldsymbol{L}}_o \quad \cdots \quad \tilde{\boldsymbol{L}}_O]^T, \\ &\boldsymbol{\mathcal{A}} = \begin{bmatrix} -2\boldsymbol{I} & \frac{2}{3}\widetilde{D}_\varpi(1,1) & \tilde{S}_\varpi(1,1) & \cdots & \tilde{S}_\varpi(1,M) \\ -2\boldsymbol{I} & \vdots & \vdots & \cdots & \vdots \\ -2\boldsymbol{I} & \frac{2}{3}\widetilde{D}_\varpi(o,1) & \tilde{S}_\varpi(o,1) & \cdots & \tilde{S}_\varpi(o,M) \\ -2\boldsymbol{I} & \vdots & \vdots & \ddots & \vdots \\ -2\boldsymbol{I} & \frac{2}{3}\widetilde{D}_\varpi(O,1) & \tilde{S}_\varpi(O,1) & \cdots & \tilde{S}_\varpi(O,M) \end{bmatrix}, \\ &\boldsymbol{x} = [\boldsymbol{L}_0 \quad C_{d_1} \quad C_{s_1} \quad \cdots \quad C_{s_M}]^T\end{aligned} \tag{23}$$

where $\tilde{\boldsymbol{L}}_o$, $\widetilde{D}_\varpi(o,m)$, $\tilde{S}_\varpi(o,m)$ are defined as follows:

$$\tilde{\boldsymbol{L}}_o = -2\boldsymbol{L}_o - W_{\varpi bkb'}\boldsymbol{\Theta}_{kbb'_o}, \tag{24}$$

$$\widetilde{D}_\varpi(o,m) = Zd_{m\varpi kb'}\boldsymbol{\Psi}_{kb'_o}, \tag{25}$$

$$\tilde{S}_\varpi(o,m) = Zs_{m\varpi bkb'}\boldsymbol{\Theta}_{kbb'_o}. \tag{26}$$

If the matrix $\boldsymbol{\mathcal{A}}$ is non-singular matrix, this normal equation can be solved, and the estimated values vector $\boldsymbol{x}$ is obtained as follows by using pseudo-inverse matrix:

$$\boldsymbol{x} = (\boldsymbol{\mathcal{A}}^T\boldsymbol{\mathcal{A}})^{-1}\boldsymbol{\mathcal{A}}^T\boldsymbol{y}. \tag{27}$$

When there are unilluminated materials during the observation term, $\boldsymbol{\mathcal{A}}$ will be a singular matrix. In this case, components for the unilluminated materials should be removed from the normal equation.

One of the advantages of a model correction by the optical property estimation is that constraints of the estimated value can be defined from physics considerations. According to the energy conservation law, the optical properties C_d and C_s have constraints as follows:

$$\begin{aligned}0 \le C_d + C_s \le 1, \\ 0 \le C_d \le 1, \\ 0 \le C_s \le 1.\end{aligned} \tag{28}$$

In addition, since C_d and C_s can be measured on ground, correctness of the estimation is assessable from the measured data. These physical senses help us to avoid misestimating and to focus on other small disturbances which usually hide amongst parameters like $c_1, c_2, \cdots$ in Eq. (5).

4. SRP Analysis Using Flight Data of PROCYON

To evaluate the accuracy, calculation cost, and correction possibility of the proposed method, an angular momentum analysis with on-orbit flight data of PROCYON was performed. This section discusses the detail and the results of the analysis.

4.1. PROCYON and observation data

PROCYON is a 50-kg class interplanetary micro-spacecraft developed by authors. PROCYON has three-axis attitude control capability and controls its own angular momentum by using a cold-gas jet reaction control system [9]. The overview of PROCYON is illustrated in Fig. 1. PROCYON has large solar panels on the +Z-axis. Depending on the sun angle, the solar panels cast shadows on side surfaces.

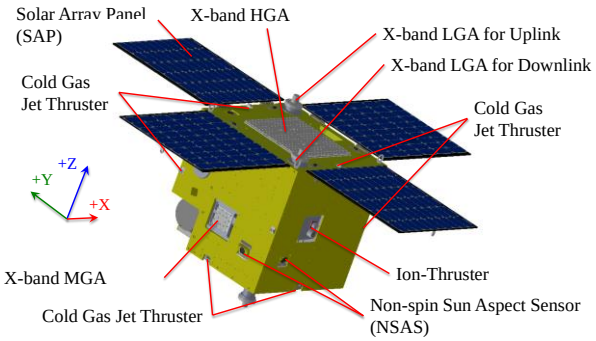

Fig. 1. Overview of PROCYON [7]

In the PROCYON mission, disturbance measurement operations were performed on orbit for accurate disturbance modelling studies. During the operations, PROCYON keeps its attitude fixing to the inertial frame and does not generate any torque from the cold-gas jet system. Therefore, the angular momentum is varied by only disturbance torque. The angular momentum is measured from the rotation speed of reaction wheels installed on PROCYON. Since the largest disturbances acting on PROCYON is SRP torque, the sun distance and the sun direction at the body-fixed frame is important for the disturbance analysis. The sun distance is given from the orbit data of PROCYON, and the sun direction is calculated from the combination of orbit data and the attitude data obtained by the on-board star sensor.

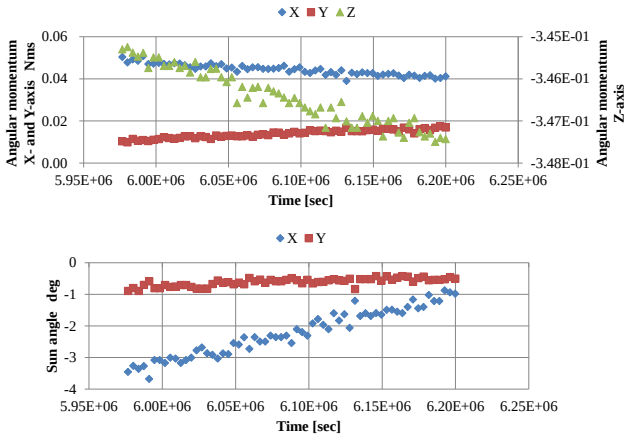

Fig. 2. Observed angular momentum and sun angle in one operation

Figure 2 shows an example of the observed angular momentum from the reaction wheels and the calculated sun direction from the orbit and attitude data. The observed data indicates the angular momentum is varied by some disturbances. In spite of the attitude is fixed to the inertial frame, the sun direction at the body frame gradually moves due to the orbital motion of PROCYON. Note that the variation of the angular momentum of Z-axis is much smaller than that of other axes because the sun direction almost aligns to Z-axis for the power generation. There is a possibility that the variation of Z-axis caused by other small disturbances (e.g., thermal radiation pressure). Here after, angular momentum of Z-axis will be ignored because this paper focuses on SRP, and it will be considered in future work.

Due to the angular momentum limitation of the reaction wheels, the maximum interval of one measurement operation is three days. After one measurement operation, the reaction wheels were desaturated by using the cold-gas jet system, and the angular momentum was changed to arbitrary initial value. After that, a new measurement operation was started. These disturbance torque measurement operations were totally performed 82 sets from May to November of 2015. The average sun angle of each measurement operation is shown in Fig. 3. The center of the figure denotes the +Z-axis of body frame. The maximum sun angle reaches to 40 deg, thus the shadowing of solar panels should be considered for accurate SRP calculation.

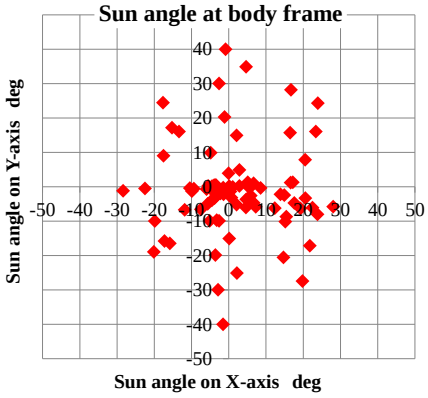

Fig. 3. Average sun angle of each operation

4.2. High-fidelity SRP model for PROCYON

In order to analyze the variation of the angular momentum of PROCYON, a high-fidelity SRP torque model was constructed by using the proposed method discussed in Section 2. In the proposed model, the three precomputed tensors $W_{\varpi bkb'}$, $Zs_{m\varpi kb'b}$, and $Zd_{m\varpi kb'}$ should be calculated before the analysis phase. They were calculated from the high-fidelity 3D geometry model of PROCYON illustrated in Fig. 4. The 3D model is constructed from real CAD and MLI design data. The geometry model has nine materials: solar cell, MLI, Ge-Kapton, and others. Their optical properties were measured on ground. The center of mass of PROCYON is given from its design information.

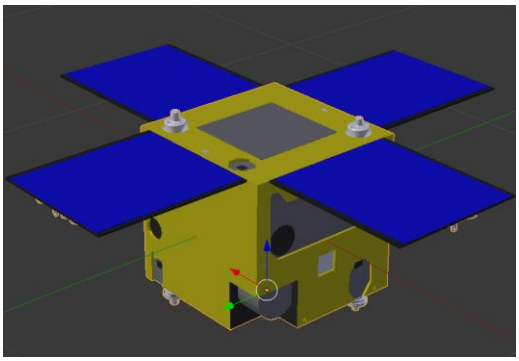

Fig. 4. High-fidelity 3D geometry model of PROCYON

For the precomputed tensor calculation, the GPU-accelerated tensor calculation tool developed by S. Ikari

et al. [6] was used. The 3D geometry model of PROCYON was divided into 235,495 micro-surfaces to express accurate shadows like Fig. 5. The divided model was input to the tensor calculation tool, and the tool generated three precomputed tensors for SRP torque calculation of PROCYON. In this study, the level-4 spherical Haar wavelet (SHW) was used for the binary visibility approximation.

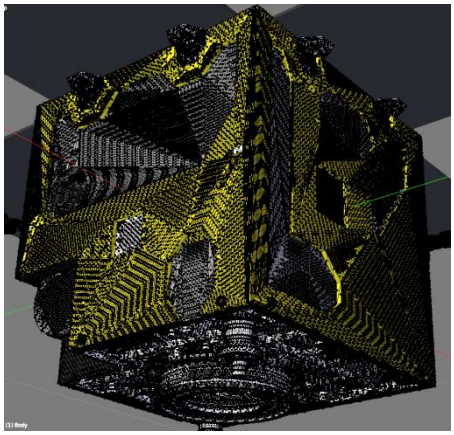

Fig. 5. Divided 3D geometry model of PROCYON (235,495 surfaces)

Table 2. Precomputation cost for PROCYON model

Calculation phase	Time [hour]
Ray-tracing for $V_p(\boldsymbol{i})$ calculation (GPU*)	7.5
$V_p(\boldsymbol{i})$ Approximation to SHW (CPU**, Matlab)	5.0
Tensor generation (CPU**, Matlab)	0.3

* NVIDIA Quadro K6000
**Intel Core i7-5930K @ 3.5GHz, 32GB RAM

Table 3. Precomputation cost for PROCYON model

File name	File size [Mbyte]
Original 3D model file (OBJ format)	10.7
$W_{\varpi kb'b}$ tensor file (Matlab format)	0.48
$Zd_{m\varpi kb'}$ tensor file (Matlab format)	2.5
$Zs_{m\varpi kb'b}$ tensor file (Matlab format)	7.4

Table 4. Calculation cost of SRP torque for one sun direction

Calculation method	Time [sec]
Ray-tracing SRP calculation (GPU*)	3.8
Proposed method (CPU**, Matlab)	0.0015

* NVIDIA Quadro K6000
**Intel Core i7-5930K @ 3.5GHz, 32GB RAM

The tensor precomputation cost is summarized in Table 2. Owing to the GPU acceleration algorithm, the precomputation for the high-fidelity PROCYON geometry model could be executed in a half day, and it is fast enough for the precomputation. Table 3 shows the data size of the precomputed tensors. The total size of the three tensors is almost same with the original 3D model size, and it is not a big issue for usual laptop computers. The calculation cost of the SRP torque is summarized in Table 4. The proposed method can calculate the SRP 2,500 times faster than the GPU ray-tracing method because of the reconstruction technique of the proposed method and the fast reconstruction property of the SHW. This reduction of the calculation cost is a great advantage of our proposed method.

4.3. Angular momentum analysis

For the evaluation of the accuracy and correction possibility of the proposed method, the observed angular momentum and the computed angular momentum from SRP models are compared. The SRP torque is calculated from the models, and the time integral of the torque is executed to obtain the angular momentum. In this paper, three types of SRP torque models were used. The first one is a simple plate model, which emulates only the +Z plane and solar panels of PROCYON. The second one is the proposed high-fidelity model with ground measured optical properties. The third one is the proposed high-fidelity model with estimated optical properties. The precomputed tensors for the second and third models are completely same. The comparison between the first and the second model shows the modelling accuracy of the proposed method, and the comparison between the second and third model reveals the effect of the optical property estimation.

The optical property estimation for the third model was performed to solve the normal equation for the linear least-squared method derived in Section 3 by using the Matlab "lsqlin" function. In this analysis, optical properties of two materials: solar cell and MLI were estimated by using all data of the 82 measurement operations, and the initial angular momentum of each operation was estimated by using the data in that operation. The total observed data is 16,400 points and the estimated data is 4 optical properties and 164 angular momentums. For the optical property estimation, constraint around the measured value was applied as follows:

$$0 \le C_{measured} - \Delta \le C_{estimated} \le C_{measured} + \Delta \le 1, \quad (29)$$

where Δ was chosen as 0.1 in this experiment.

The results of the angular momentum analysis of PROCYON are shown in Fig. 6. This figure presents the standard deviation (STD) of angular momentum error between the observed value and the integrated value of the SRP torque obtained from the three models. The comparison between the plate model and the proposed model with measured optical property shows that the proposed model is more accurate than the simple plate model, in particular at the large sun angle cases. This result verifies the good accuracy of the proposed method. The comparison between the proposed method with measured optical property and that with the estimated one shows that the accuracy of the SRP torque model was improved by the optical property estimation. The model correction seems like success since the accuracy was improved; however, the optical property estimation was not good enough. Table 5 summarizes the results of the estimation. All estimated optical properties are stick to the limitation of the constraint of $\Delta = 0.1$. These differences between measured and estimated value is too large to be explained by ground measurement uncertainties. It is thought that PROCYON received torque which is not modeled in the proposed method, for example, thermal radiation pressure or the mismodeling in the geometry model. These mismodeling issues occur not only for the proposed method but also other

SRP calculation methods. One of the advantages of the proposed method is that some misestimation can be detected from the physical sense of optical properties. Thus, the proposed method may be useful for practical accurate SRP analyses, and it can be improved by including other disturbance models.

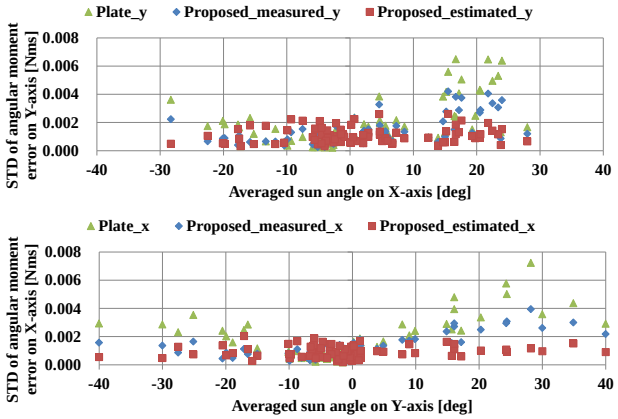

Fig. 6. Standard deviation of angular momentum for three SRP models

Table 5. Summary of the optical property estimation

	Measured		Estimated	
Materials	C_d	C_s	C_d	C_s
MLI	0.03	0.60	0.13	0.50
Solar cell	0.006	0.08	0.106	0.17

5. Conclusions

This paper proposes an accurate, fast, and model correctable SRP calculation method for practical astrodynamics analyses. The key techniques of the proposed method are decomposition and reconstruction of three components of the SRP calculation: spacecraft geometry, material property, and sun information. The proposed method precomputes and approximates the binary visibility function which represents shadows on surfaces. The precomputation and the approximation allow us to use the tensor calculus rules for the high-fidelity SRP calculation. According to the tensor calculus, the three components were decomposed and reconstructed based on material groups. The reconstructed SRP equation includes three precomputed tensors which are obtained by using only the spacecraft geometry. Owing to the precomputed tensors, the calculation cost of the proposed SRP equation no longer depends on the number of micro-surfaces, and the real time calculation cost is dramatically decreased. Furthermore, a normal equation of the linear least-squared method to estimate the optical properties was derived from the reconstructed SRP equation.

In order to evaluate the accuracy, calculation cost, and correction possibility of the proposed method, an angular momentum analysis with on-orbit flight data of interplanetary spacecraft PROCYON was performed. The precomputed tensors were generated from the high-fidelity 3D model of PROCYON in a half day, which is a practical precomputation time. It was verified that the real time calculation cost of the proposed method is much faster than that of GPU-accelerated ray-tracing method. The accuracy of the proposed method is also better than the simple model which ignores shadow effect. In addition, the optical property estimation improved the final accuracy of the angular momentum; however, it is though that the estimated optical properties include some effects of other small disturbances or geometric mismodeling.

The issues revealed in the optical property estimation will be occurred in conventional simple estimation methods. Because our proposed method is more accurate than the conventional estimation methods, the proposed method may be useful for practical accurate SRP analyses such as a precise orbit determination of navigation satellites or an attitude stability analysis of deep space probes. The improvement by including thermal radiation pressure or structural mismodeling effect will be considered in future work.

Acknowledgments

The authors would like to express their deepest gratitude to all members of PROCYON project team. This work was supported by JSPS Grant-in-Aid for JSPS Fellows Number 14J03417.

References

[1] M. Ziebart, "High Precision Analytical Solar Radiation Pressure Modeling for GNSS Spacecraft," the University of East London for the degree of Doctor of Philosophy, 2001.

[2] E. Doornbos, "Modeling of non-gravitational forces for ERS-2 and ENVISAT," Delft University of Technology, Delft, Netherlands, 2001.

[3] M. Ziebart, "Analytical solar radiation pressure modelling for GLONASS using a pixel array," *Journal of Geodesy*, vol. 75, no. 11, pp. 587-599, 2001.

[4] C. J. Rodriguez-Solano, U. Hugentobler and P. Stergenberger, "Adjustable box-wing model for solar radiation pressure impacting GPS satellites," *Advances in space research*, vol. 49, no. 7, pp. 1113-1128, 2012, doi: 10.1016/j.asr.2012.01.016.

[5] S. Ikari, T. Ebinuma, R. Funase and S. Nakasuka, "A Novel Semi-Analytical Solar Radiation Pressure Model with the Shadow Effects for Spacecraft of Complex Shape," in *26th Space Flight Mechanics Meeting*, Napa, CA, USA, 2016.

[6] S. Ikari, K. Tokunaga, T. Ebinuma, R. Funase and S. Nakasuka, "A Study of Shadow Representation for High-fidelity Solar Radiation Pressure Calculation," in *AIAA SPACE 2016 Astrodynamics Specialist Conference*, Long Beach, CA, USA, 2016.

[7] R. Funase, H. Koizumi and S. Nakasuka, "50kg-class Deep Space Exploration Technology Demonstration Micro-Spacecraft PROCYON," in *28th Annual AIAA/USU Conference on Small Satellites*, Utha, 2014.

[8] P. Schröder and W. Sweldens, "Spherical Wavelets: Efficiently Representing Functions on the Sphere," in *Computer Graphics Proceedings (SIGGRAPH 95)*, 1995.

[9] S. Ikari, T. Nakatani and et al., "Attitude Determination and Control System for the Micro Spacecraft PROCYON," in *30th ISTS*, Kobe, Japan, 2015.